







# Advanced Imaging of Gout and Other Inflammatory Diseases Around the Knee

Iwona Sudół-Szopińska, Prof., MD, PhD<sup>1</sup>  Michał Lanckoroński, MD<sup>1</sup>   
 James Teh, BSc, MBBS, MRCP, FRCR<sup>2</sup>  Torsten Diekhoff, MD<sup>3</sup>  Chiara Giraudo, MD, PhD<sup>4</sup>   
 Snehanish Roy Chaudhary, MBBS, MSc, MRCS, FRCR<sup>2</sup> 

<sup>1</sup> Department of Radiology, National Institute of Geriatrics, Rheumatology and Rehabilitation, Warsaw, Poland

<sup>2</sup> Department of Radiology, Nuffield Orthopaedic Centre, Oxford University Hospitals NHS Trust, Oxford, United Kingdom

<sup>3</sup> Department of Radiology, Charité - Universitätsmedizin Berlin, Campus Mitte, Humboldt-Universität zu Berlin, Freie Universität Berlin, Berlin, Germany

<sup>4</sup> Department of Cardiac, Thoracic, Vascular Sciences and Public Health – DCTV, University of Padova, Padova, Italy

Address for correspondence Prof. Dr. Iwona Sudół-Szopińska, MD, PhD, Department of Radiology, National Institute of Geriatrics, Rheumatology and Rehabilitation, Warsaw 02-637, Poland (e-mail: sudolszopinska@gmail.com).

Semin Musculoskelet Radiol 2024;28:337–351.

## Abstract

The knee is one of the most commonly affected joints in the course of inflammatory arthropathies, such as crystal-induced and autoimmune inflammatory arthritis. The latter group includes systemic connective tissue diseases and spondyloarthropathies. The different pathogenesis of these entities results in their varied radiologic images. Some lead quickly to joint destruction, others only after many years, and in the remaining, destruction will not be a distinguishing radiologic feature.

Radiography, ultrasonography, and magnetic resonance imaging have traditionally been the primary modalities in the diagnosis of noninflammatory and inflammatory arthropathies. In the case of crystallopathies, dual-energy computed tomography has been introduced. Hybrid techniques also offer new diagnostic opportunities. In this article, we discuss the pathologic findings and imaging correlations for crystallopathies and inflammatory diseases of the knee, with an emphasis on recent advances in their imaging diagnosis.

## Keywords

- ▶ knee
- ▶ imaging
- ▶ gout
- ▶ rheumatoid arthritis
- ▶ spondyloarthropathy

The knee is frequently affected by various inflammatory diseases, such as crystallopathies, like gout, as well as autoimmune and autoinflammatory arthritides, such as rheumatoid arthritis (RA), juvenile idiopathic arthritis (JIA), and spondyloarthropathies (SpA). These conditions present distinct radiologic features. For instance, RA often leads to rapid joint destruction, whereas in others, like gout, the damage to joints may take years. Historically, the diagnosis relied on radiography, ultrasonography (US), and magnetic resonance imaging (MRI). For crystallopathies, dual-energy computed tomography (DECT) is now also used. Recent advances have introduced hybrid techniques, enhancing early diagnosis, prognostication, and treatment monitoring.

## Advancements in Imaging Modalities

### Ultrasonography

Knee US has traditionally been the initial examination in the diagnostic pathway of inflammatory arthropathies, often following a radiographic examination. Its primary role is in the early diagnosis, monitoring of treatment, and guiding interventions. The strength of US is its ability to evaluate soft tissues in detail including the joint, tendons, and ligaments. Doppler interrogation allows a real-time assessment of synovial inflammation.

Examination of the knee is usually performed with a high-frequency US transducer, generally 5–18 MHz, that provides superior spatial resolution of superficial tissues.<sup>1</sup> Recent

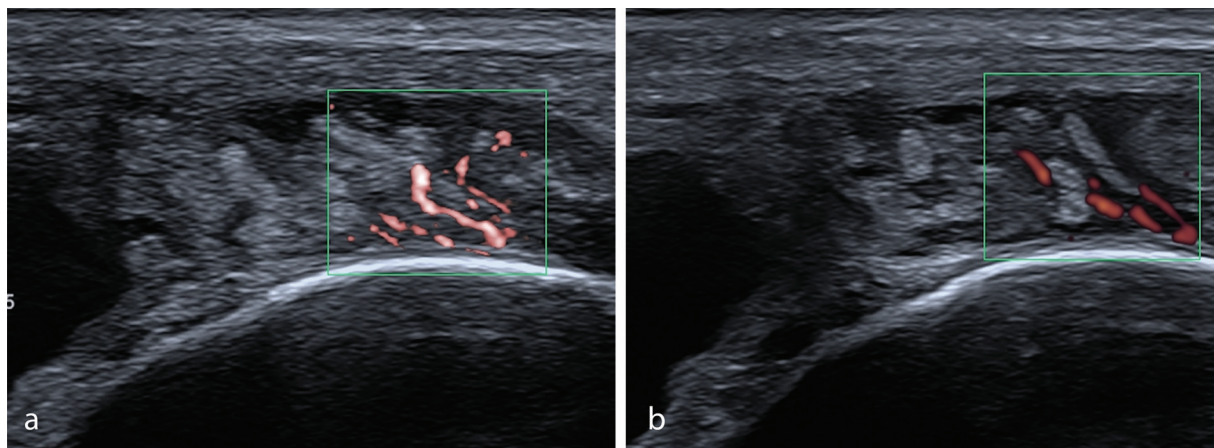


**Fig. 1** A 51-year-old man with rheumatoid arthritis: knee joint effusion, synovial thickening, and vascularization. More vessels are seen using (a) microflow imaging than (b) power Doppler.

advances in US include high-frequency transducers of 20 to 50 MHz for the assessment of musculoskeletal (MSK) tissues and newer technologies such as microflow imaging and soft tissue elastography.<sup>1</sup>

Microflow imaging has been a breakthrough in the diagnosis of inflammatory arthropathies, specifically RA<sup>2</sup> and JIA.<sup>1</sup> Its sensitivity surpasses traditional methods like power Doppler and color Doppler because it can detect even small vessels without the need for administering contrast<sup>2</sup> (→**Fig. 1**). The advantages of this technique include the assessment of blood flow in the microvasculature, effective separation of flow signals from tissue motion artifacts, high resolution of images, minimal motion artifact, and high frame rates.<sup>2</sup>

Superb microflow imaging (SMI) can be performed in either standard color or even more sensitive monochrome mode where the background signals are subtracted and only vessels, including those with the lowest velocity flow, are seen.<sup>2</sup> A quantitative image analysis is achievable using vascular index software that allows the operator to set a region of interest (ROI) of a different size in a two-dimensional (2D) static image and automatically calculate the number of color pixels of vascular signal within all pixels of the ROI.<sup>1,2</sup> SMI may significantly improve patient management at the stage of initial diagnosis, follow-up, and remission.<sup>1</sup>

In MSK radiology, application of quantitative contrast-enhanced US is limited mainly to the evaluation of muscle and tendon perfusion, or soft tissue tumors in the context of research.

Elastography can assess tissue stiffness. It is particularly useful to evaluate superficial tissues (skin, subdermis, fascia, muscles, and tendons) in juveniles and adults with scleroderma, polymyositis, and dermatomyositis<sup>1,2</sup> (→**Fig. 2**). The two types of elastography are strain and shear-wave elastography (SWE). The latter is an objective quantitative technique that measures the absolute elasticity value of soft tissues.<sup>2</sup> It uses an acoustic radiation force pulse sequence to generate shear waves that propagates through the tissues perpendicular to the US beam, causing transient displacements.<sup>1</sup>

SWE images are automatically coregistered with standard B-mode images to provide quantitative color elastograms with anatomical specificity. Shear waves propagate faster through stiffer and inflamed tissues, as well as along the long axes of tendons and muscles.<sup>1</sup> In rheumatology, SWE has mainly been used to evaluate tendon and muscle pathology, presenting shear waves velocity differences depending on the disease activity.<sup>1,2</sup> For example, softening of the patellar tendon in the course of arthritis was reported in the literature.<sup>1</sup>

### Magnetic Resonance Imaging

MRI enables comprehensive assessment of soft tissues, cartilage, and bone marrow. Its high contrast resolution and multiplanar capability allows the identification of early inflammatory changes and treatment monitoring.<sup>3</sup> Unlike US, MRI can visualize the bone marrow and provide access to all structures of the joint.

In the last few decades, novel MRI techniques have emerged: a robust fat suppression (FS) technique using chemical shift imaging (CSI), diffusion-weighted imaging (DWI), advanced quantitative MRI techniques, such as T2 mapping and T1ρ mapping, dynamic contrast-enhanced MRI (DCE-MRI), diffusion tensor imaging, and whole-body MRI (WB-MRI).<sup>4–6</sup>

Robust FS techniques predominantly involve Dixon sequences that use CSI. They take advantage of the slight difference in resonance frequency between water and fat protons to provide a series of four sets of images: in-phase (IP), out-of-phase (OP), water only, and fat only.<sup>4</sup> Although Dixon described it in the 1980s, it has only recently become possible to associate this method with spin-echo (SE)-based sequences, the backbone of MSK MRI protocols, opening the door for multiple applications in this field. CSI MRI can also be used to probe bone marrow fat content quantitatively, by measuring the signal drop between IP and OP images or by calculating the fat fraction. This can be done both on gradient-echo (GRE) and SE sequences.<sup>4</sup>

The Dixon method has proven to be more robust to magnetic field inhomogeneities than chemical shift selective

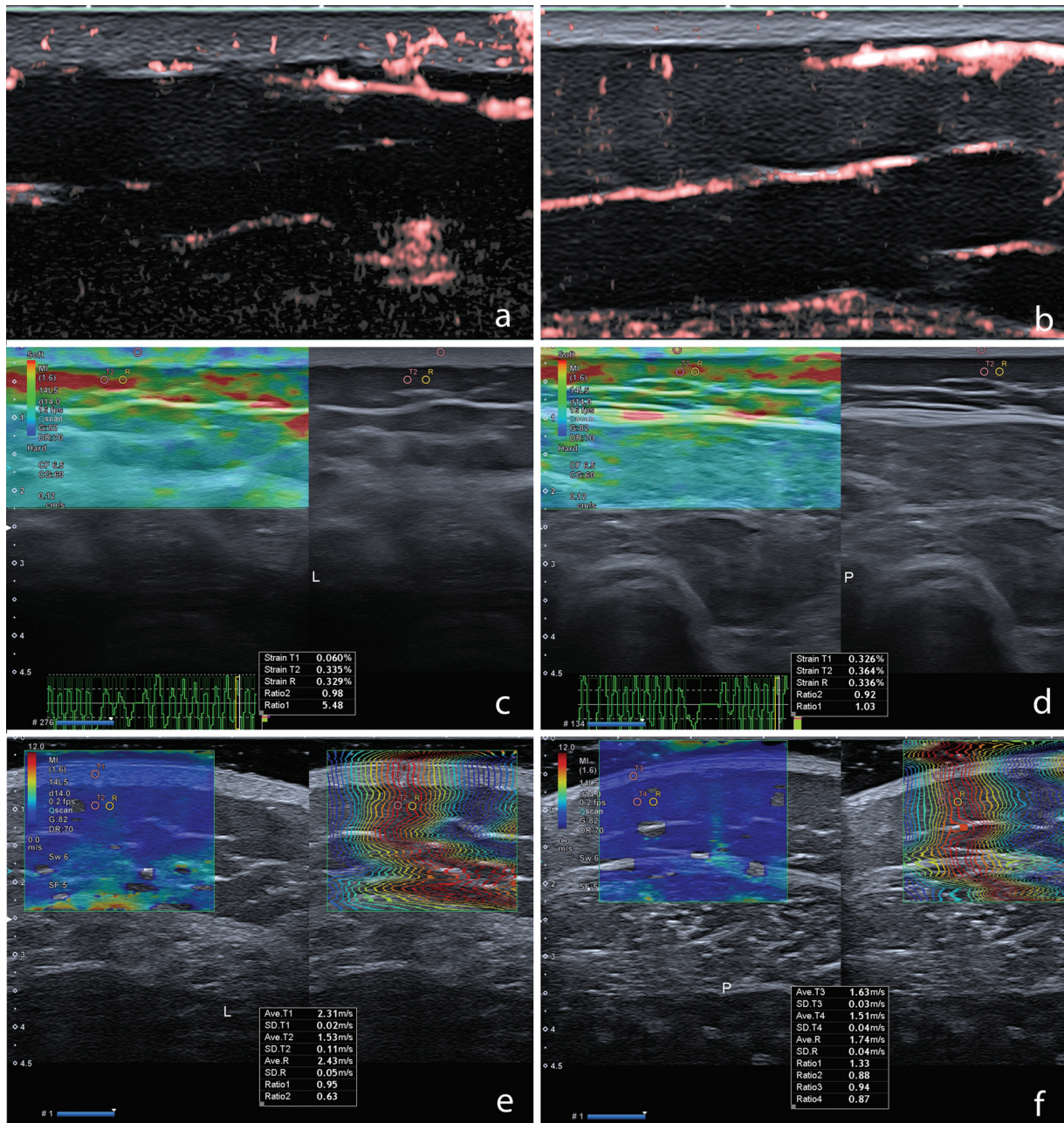


**Fig. 2** A 6-year-old boy with localized scleroderma with skin hardening on the lateral side of the left thigh. (a) Superficial tissue evaluation with 24 MHz transducer shows skin thickening with increased vascularity in superb microvascular imaging on the affected left side that confirms active lesions. (b) Normal skin thickness, echogenicity and vascularity of the contralateral right thigh. (c,d) Compression elastography confirms skin stiffness of the affected left (L) side in comparison to the right (P) side. (e, f) Shear-wave elastography confirms skin stiffness on the affected left (L) side, in comparison the normal right thigh (f).

suppression while providing a better signal-to-noise ratio than short tau inversion recovery sequences.<sup>4</sup> Therefore, it is an appealing technique for large field-of-view (FOV) imaging of the bone marrow, whereas in knee assessment its use is generally reserved to assess tumors rather than inflammatory conditions. The robust FS and reduced examination time are additional advantages of Dixon acquisitions.

DWI is based on the diffusion of water molecules in tissues and obtained by two symmetrical gradient pulses on conventional MR sequences, the first causing the phase shift of water molecules and the second one canceling it<sup>6</sup> (► Fig. 3). It has not gained popularity, despite reports of comparable accuracy in

diagnosing synovitis and predicting radiologic and clinical response in patients with JIA.<sup>6-8</sup> Some challenges associated with this technique include long study time, high sensitivity to field inhomogeneities, the need for strong gradients, and subjectivity in positioning the ROIs that hampers the objective quantification of disease.<sup>6</sup> Nevertheless, some potential solutions to resolve this shortcoming have already been proposed.<sup>6</sup>

Intravoxel incoherent motion (IVIM) is a method developed by Le Bihan and colleagues in 1988 to evaluate the microscopic motion of water molecules that simultaneously quantifies diffusion and microperfusion using diffusion-weighted sequences.<sup>6</sup> Since then, IVIM has been applied in

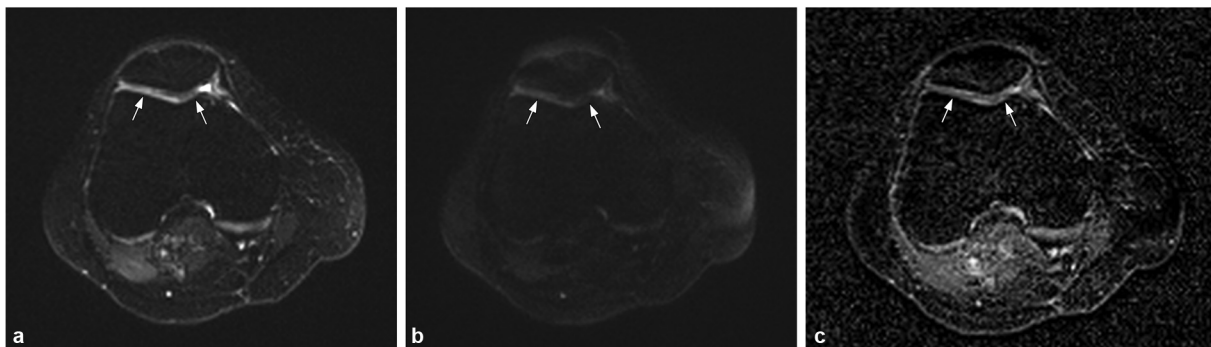


**Fig. 3** Axial RESOLVE Diffusion Weighted Imaging (TR 4710, TE 71, number of averages 2, slice thickness 3.5 mm) of the knee demonstrating the thin, irregular and inhomogeneous cartilage of the patellofemoral compartment (white arrows on the b50 s/mm<sup>2</sup> and b800 s/mm<sup>2</sup> images, and on the apparent diffusion coefficient map respectively in a, b, and c).

various fields including rheumatology, with very good results.<sup>6</sup>

Quantitative assessment of synovial vascularization on DCE-MRI can evaluate the degree of synovial inflammation.<sup>9</sup> DCE-MRI consists of assessing tissue perfusion through serial acquisitions of images before and after a bolus of intravenous contrast injection and the review of the variation of MR signal intensity of the tissues of interest, both qualitatively and quantitatively,<sup>4</sup> using T1-weighted GRE sequences that allow a high temporal resolution (1–10 s).<sup>6</sup> These generate signal intensity curves based on the distribution of contrast medium in the intra- and extravascular spaces, from which quantitative perfusion parameters can be extracted by applying a pharmacokinetic or a heuristic approach.<sup>6</sup>

The important role of DCE-MRI for assessing synovitis in the knee joint is well established, especially in patients with early disease not diagnosed by conventional MRI.<sup>6</sup> DCE-MRI may even eventually replace the semiquantitative Rheumatoid Arthritis Magnetic Resonance Imaging Score (RAMRIS).<sup>6</sup> Encouraging results in this direction emerged from an exploratory study about the effect of tofacitinib, in which both DCE-MRI with heuristic analysis and a novel quantitative adaptation of the RAMRIS, based on active appearance modeling, called

Rheumatoid Arthritis Magnetic Resonance Imaging Quantification (RAMRIQ), were applied, showing an early response to treatment.<sup>6</sup>

Several new techniques are used for cartilage assessment (►Fig. 4). T1ρ is a technique sensitive to low-frequency interactions of macromolecular protons and bulk water.<sup>6</sup> T1ρ relaxation time describes spin-lattice relaxation in the rotation frame in the presence of an external radiofrequency pulse in the transverse plane. Images acquired with different spin-lock frequencies are used for the calculation of T1ρ in each pixel by fitting a signal to exponential function.<sup>6</sup>

Similarly, in T2 mapping, which maps the transversal relaxation constant, T2 values are calculated from a multi-echo multislice sequence by fitting a signal with the exponential curve.<sup>6</sup> In patients with RA, T1ρ and T2 values of the knee cartilage were higher than in healthy volunteers except for the patella and lateral tibial plateau.<sup>6</sup> Similar results using T1ρ were achieved on tissue samples of 5 and 14 patients, respectively, with RA and osteoarthritis (OA) who underwent total knee arthroplasty.<sup>6</sup> The authors demonstrated that T1ρ is useful to detect and map early stages of cartilage degradation in both diseases and that changes due to RA are associated with higher T1ρ values.<sup>6</sup>

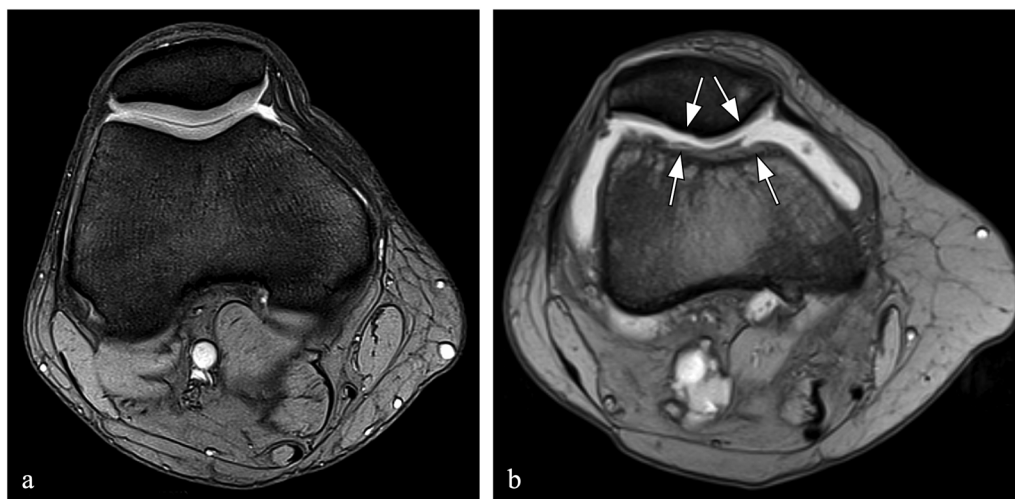


**Fig. 4** Axial Multiple Echo Data Image Combination (MEDIC), T2\*-weighted spoiled gradient-echo sequence of the knee nicely showing (a) patellofemoral cartilage with regular thickness and signal intensity in a 47-year-old male patient. (b) Cartilage loss with irregular margins (white arrows) in a 70-year-old woman with severe osteoarthritis.

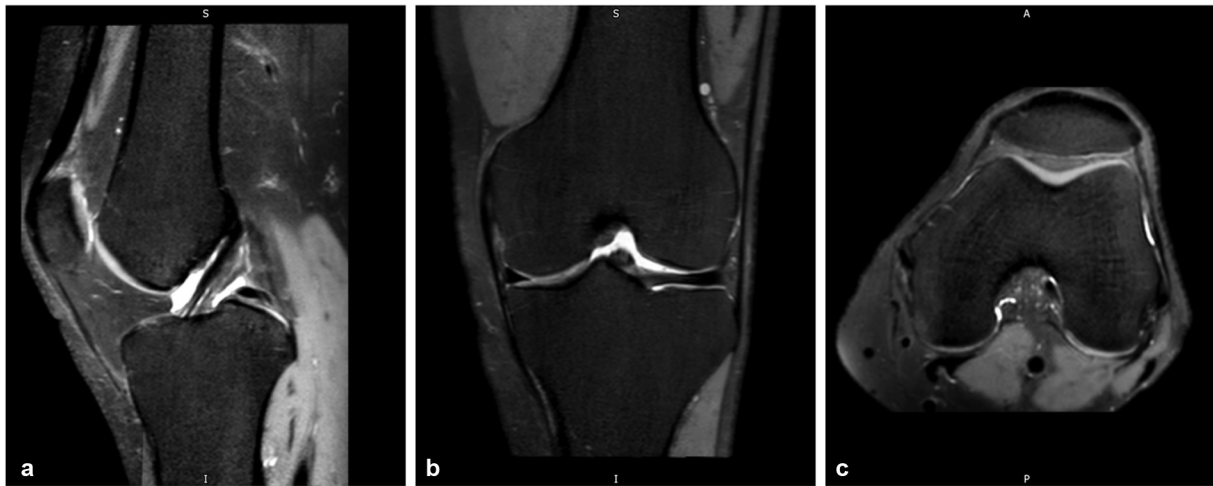


**Fig. 5** Isotropic knee images, proton-density fat suppression sequence with 0.8-mm slice thickness, and 0.4-mm spacing, TR: 1,000 ms, TE: 50 ms, flip angle: 90 degrees. (a) Sagittal image, which is the original scan plane. (b) Coronal image, reformatted from the sagittal plane data set. (c) Axial image, reformatted from the sagittal plane data set.

Delayed gadolinium-enhanced MRI of cartilage (dGEMRIC) allows the indirect quantification of glycosaminoglycans after the injection of gadolinium diethylenetriamine-penta-acetic acid (Gd-DPTA<sup>2</sup>) in areas affected by cartilage loss. Typically, low dGEMRIC indexes are seen in RA.<sup>6</sup> The ultrashort echo time and the zero echo time MRI sequences in the knee allow the detection of rapidly decaying transverse magnetization in the so-called short T2 tissues such as cartilage, fibrocartilage (menisci), cortical bone, and tendons.<sup>6</sup>

Three-dimensional (3D) isotropic MRI acquisitions have several advantages over 2D MRI<sup>10</sup> (►Fig. 5). 3D MRI provides improved spatial resolution and can generate high-quality reformats from the original data set.<sup>10</sup> Thin continuous slices improve through-plane resolution that reduces artifacts from partial-volume averaging, can delineate erosive changes and synovitis better than 2D images,<sup>10</sup> and enhances the ability to delineate more subtle pathologies that might be undetectable with conventional 2D MRI.<sup>10</sup> The 3D isotropic MRI pulse sequences allow reformatting of the high-quality images in any desired plane to improve image assessment,<sup>10</sup> whereas the ability to reformat images from a single data set can reduce the number of sequences and decrease scan time.<sup>10</sup>

The 2D and 3D GRE sequences with different types of contrast weighting can be broadly classified into two categories: dark fluid signal sequences and bright fluid signal sequences<sup>11</sup> (►Fig. 4). Research on bright and dark fluid GRE sequences in knee MRI has focused mainly on cartilage evaluation because there is typically good contrast between fluid, articular cartilage, and bone.<sup>11</sup> High-resolution isotropic dark fluid GRE morphological sequences have often been considered the standard for cartilage morphology assessment in the research setting,<sup>11</sup> but they can have long scan times, forcing a compromise of resolution or quality when optimized for clinically feasible acquisition times. Bright fluid high-resolution 3D GRE sequences, such as the 3D double-echo steady-state sequence, offer faster acquisition times and favorable fluid-to-cartilage contrast, resulting in improved assessment of the cartilage surface.<sup>11</sup>

### Dual-Energy Computed Tomography

Computed tomography (CT) with its multiplanar capability and excellent depiction of bone is the best method to assess erosions.<sup>12</sup> However, due to radiation concerns, it is infrequently used solely for this purpose. Spectral CT operates on the principle that tissue attenuation is influenced not just by density but also by the atomic number (Z) and the photon beam's energy.<sup>4</sup> By leveraging these properties, spectral CT can characterize and quantify specific tissue components.<sup>4</sup>

The most prevalent subset of spectral CT is DECT, using two distinct X-ray energy spectra.<sup>4</sup> In dual-source DECT, two tube-detector pairs are utilized, with adjustable tube voltages, facilitating fast single energy combinations. The two separate tubes are offset by ~90 degrees to each other, contributing to the material decomposition performed only on the image domain due to the spatial offset between acquisitions.<sup>13</sup>

One technique for single-source DECT is rapid kilovoltage switching. In those scanners, there is virtually no temporal mismatch and full FOVs with the X-ray tube switching between 80 and 140 kVp in <0.2 ms.<sup>13</sup> Contrary to dual-source DECT systems, the resulting projection-space decomposition offers greater flexibility in the types of materials that can be used for data and provides a significant advantage in minimizing beam-hardening artifacts.<sup>13</sup>

Other kinds of DECT techniques include dual-layer technology, sequential acquisitions, or split-filter approaches. Recent innovations have introduced photon-counting detectors, groundbreaking technology that enables multi-energy imaging, through direct counting of individual incoming photons and measurement of their energy level.<sup>4</sup> These detectors offer superior spatial resolution, dose reduction, and enhanced material differentiation, and they are less susceptible to beam-hardening artifacts.<sup>4,13</sup>

These special CT techniques offer material characterization based on two or more X-ray photon energy-dependent attenuations.<sup>6</sup> The distinct absorption properties of calcium and urate have positioned DECT as the leading technique for

gout investigation, even in its early stages.<sup>6,14</sup> This allows for both qualitative and quantitative determination of monosodium urate (MSU) deposition in joints and tissues and resulted in high sensitivity (88%) and specificity (90%) in a meta-analysis.<sup>6,15</sup> After the acquisition scan, with a protocol optimized for detecting small urate deposits, the data sets allow for the characterization and quantification of different materials and structures, such as urate deposits and soft tissues.<sup>6</sup> This is achieved by color-coding features on 3D multiplanar volumetric images. DECT excels in visualizing deeper or intricate structures and in displaying the anatomical extent of gouty deposits.<sup>13</sup> Artifacts produced during DECT scanning and postprocessing can lead to false-positive results. The common artifacts encountered in DECT are well known.<sup>13</sup>

Pseudogout, another acute inflammatory monoarticular crystal arthropathy characterized by the deposition of calcium pyrophosphate dihydrate crystals, can present similarly to gout on radiographs, US, or CT. DECT can diagnose pseudogout by revealing the presence of calcium and the absence of MSU crystals.<sup>16</sup> The sensitivity of DECT in detecting pseudogout is thus lower than that for gout detection because it is a diagnosis of exclusion.<sup>16,17</sup>

Other application of DECT around the knee include bone marrow imaging.<sup>16</sup> By using virtual non-calcium (VNCa) reconstructions, DECT can detect nontraumatic bone marrow edema (BME) of the hip and knee with high sensitivity and specificity.<sup>4</sup> Therefore, if MRI is contraindicated, DECT can help depict BME associated with cortical erosions, confirming osteomyelitis. In inflammatory arthropathies, VNCa images can evaluate osteitis in the form of BME, correlating well with MRI.<sup>16</sup>

Finally, regarding metals, DECT is a validated technique for metal artifact reduction and also used to diagnose iron-containing entities. It can characterize and color-code iron, which can be used to diagnose synovial giant cell tumors. This benign neoplastic disorder is characterized by hemosiderin deposition, along with mononuclear cells and multinuclear giant cells. In patients with soft tissue masses around the joint, the presence of iron at DECT is indicative of this disease.<sup>16</sup> DECT can also be used in metallosis to detect metal debris and pseudotumors.<sup>16</sup>

### Nuclear Medicine and Molecular Imaging

Nuclear imaging relies on the intravenous injection of radiopharmaceuticals to assess the distribution of hematopoietic or reticuloendothelial cells.<sup>4</sup> Imaging of the hematopoietic component can be achieved by white blood cell (WBC) scintigraphy, by injecting the patient's WBCs after they have been radiolabeled in vitro with technetium (Tc)-99m or indium-111, or by injecting Tc-99m-labeled mouse anti-granulocytes monoclonal antibodies or antibody fragments.<sup>4</sup> The most common indication for WBC imaging in the knee is to assess a periprosthetic infection and to differentiate it from mechanical loosening.

Bone scintigraphy with intravenous injection of Tc-99m-labeled diphosphonates allows imaging of osteoblastic activity.<sup>4</sup> In rheumatology, they are used to diagnose insufficiency

fractures, although the knee is not a predilection area for that pathology.

Radiosynovectomy (RSV) is a treatment that destroys the hypertrophic synovial membrane using ionizing radiation. It requires the application of  $\beta$ -emitting radionuclides to treat the chronic inflammation of the joints.<sup>18</sup> For the knee and other large joints, the procedure is performed using an intra-articular injection of yttrium-90 silicate/citrate. RSV is an overall safe technique with known contraindications.<sup>18</sup> Despite the use of ionizing radiation, overall exposure is low, and no evidence indicates an increase in cancer risk when compared with the general population in adult patients.<sup>18</sup>

### Hybrid Imaging

Single-photon emission computed tomography (SPECT), positron emission tomography (PET)/CT, and PET/MRI provide functional and improved 3D anatomical depiction of inflammatory lesions, enabling semiquantitative evaluation of uptake and metabolism of radiotracers (in SPECT) or isotopes of glucose in inflammatory cells (PET). PET/MRI provides the simultaneous acquisition of metabolic information combined with the intrinsic high soft tissue contrast of MRI and the lower radiation dose, which has expanded its use in the MSK field.<sup>6</sup> PET/MRI offers several advantages over PET/CT, including a reduced radiation burden for the patient, superior soft tissue contrast, and better coregistration of PET data with MRI-based motion correction.<sup>19</sup>

The benefits of PET/CT have been widely described in rheumatology.<sup>6</sup> This hybrid technique allows not only a visual assessment of the affected areas but also a (semi)quantitative evaluation of the inflammatory process, using parameters like SUVs (i.e., SUV<sub>max</sub> and SUV<sub>mean</sub>), metabolic active volume, and total lesion glycolysis.<sup>6</sup> In terms of radioactive labels, fluorine-18 fluorodeoxyglucose (18F-FDG) and 18F-sodium fluoride (18F-NaF) are the most commonly applied tracers in clinical practice for inflammatory arthritis.<sup>6</sup>

FDG-PET/CT has been proposed as an objective noninvasive adjunct to the clinical assessment of patients with RA, contributing to both the initial diagnosis and the response to treatment.<sup>19</sup> PET has also been used as a tool to assess progressive joint destruction in patients with RA. The degree of hypermetabolism in joints with active destruction is higher than that in joints with only nondestructive inflammation. Baseline or pretreatment SUV<sub>max</sub> is a significant predictive factor of large joint destruction at 2 years.<sup>19</sup> Follow-up FDG-PET/CT was also shown to be an effective tool in monitoring the response to treatment of RA and other arthropathies.<sup>19</sup>

Although not commonly affecting knees, in polymyalgia rheumatica (PMR) FDG-PET/CT was found useful to differentiate this entity from the onset of RA in older adults.<sup>19</sup> FDG-PET/CT has also been shown to be beneficial for monitoring response to treatment in patients with PMR.

FDG-PET has shown promise as an adjunct to clinical assessment in spondyloarthropathies. In a study of seven patients with ankylosing spondylitis, three patients with psoriatic arthritis, and one patient with nonspecific SpA, FDG-PET accurately delineated the inflammatory activity at

both articular and extra-articular sites.<sup>19</sup> The uptake in the affected joints in these patients with SpA was nonsymmetrical and heterogeneous (compared with the relatively symmetrical findings in RA). There was intense tendinous, enthesal, and muscular uptake at symptomatic joints.<sup>19</sup>

### Overview of Pathologic Findings in Arthropathies

Inflammatory rheumatic diseases affecting the knee joint predominantly exhibit synovitis, frequently accompanied by effusion, that will lead to joint damage. Other tissues affected by inflammatory conditions around the knee include bursae, tendons, entheses, bone marrow, fat tissue, muscles, fascia, and superficial tissues, like skin and the subdermis.

Gout and other inflammatory arthropathies can lead to affliction of the knee extensor apparatus, notably of the deep infrapatellar bursa and the gastrocnemius bursa. The same entities can induce tenosynovitis and tendinopathy, as well as enthesopathy, with gout showing a predilection for impacting the extensor side of the knee<sup>20</sup> and SpA in general showing predilection to lower limbs entheses, causing enthesitis, a hallmark of SpA in the knee.

The concept of the “enthesis organ” suggests that tissues adjacent to the enthesis, such as fatty tissue, bursa, and bone marrow in the bony part of an enthesis, may also experience inflammation.<sup>21</sup> However, degenerative enthesopathic findings, especially in the lower limb, are more prevalent, requiring a cautious diagnosis to avoid misattributing inflammatory arthritis based solely on imaging findings.<sup>22</sup> The criteria to differentiate inflammation-related enthesitis from metabolic, age, and overload-driven enthesopathy remain to be solidly established.<sup>22,23</sup>

In the popliteal fossa, some tendons (most often the semi-membranous) may be involved by different processes, including tenosynovitis, tendinopathy, bursitis, and enthesitis.

In the course of most of the presented diseases, the intra-articular and periarticular fat tissue may also look abnormal on US and MRI because it can become a site of inflammatory infiltration, in addition to synovium and subchondral bone marrow, with cells pivotal in joint destruction.<sup>24</sup>

Gout and inflammatory arthropathies can lead to knee damage, then erosions (marginal, later subchondral), articular cartilage damage (resulting in osteochondral lesions and secondary OA), and knee malalignment, as well as proliferative changes, like enthesophytes and periosteal ossifications (characteristic of SpA).

Whereas US allows intra- and extra-soft tissue assessment (except for deep intra-articular structures), MRI is optimal for imaging cartilage and may also reveal BME, signaling cellular infiltration, considered a pre-erosive condition and a response-to-treatment biomarker.

MRI also offers a superior assessment of the menisci and reveals frequent infiltration and damage by synovium in RA, whereas JIA patients often present with meniscal hypoplasia.<sup>25</sup>

Osteophytes and subchondral sclerosis stand out as distinctive features of OA that may manifest secondarily to inflammatory arthritis.

Additionally, rheumatic diseases, such as scleroderma, dermatomyositis, and polymyositis, exhibit a propensity to involve the knee, particularly affecting soft tissues (skin, subdermis, fascia, muscles) (►Fig. 2).

Rheumatoid nodules, emerging under the skin, are observed in up to 20% of RA patients, predominantly appearing in areas subjected to trauma or friction.

### Specific Forms of Arthropathies

Although the individual diseases and arthropathies described here can have multifactorial etiologies with complex and overlapping pathogeneses, the specific forms of arthropathies can be broadly classified (►Table 1). In this review, we focus on gout and RAs, which after septic arthritis are the most important arthropathies to exclude in the knee joint. Brief overviews of other connective tissue diseases (JIA, Still’s disease, scleroderma, SpA, and chronic nonbacterial osteitis) are also provided.

#### Gout

Gout is the most common form of inflammatory arthropathy resulting from MSU crystal deposition, and its prevalence is increasing in Western societies.<sup>13,26,27</sup> The knee, following the metatarsophalangeal joints, is the second most common location affected by gout.<sup>26</sup> If left untreated, the persistent deposition of MSU crystals in the joints and surrounding soft tissues can lead to progressive joint destruction.<sup>13</sup>

**Table 1** Classification of arthropathies

<b>Crystal:</b> <ul style="list-style-type: none"> <li>• Gout</li> <li>• CPPD                             <ul style="list-style-type: none"> <li>◦ Pyrophosphate arthropathy</li> <li>◦ Pseudogout</li> </ul> </li> <li>• Other crystals (e.g., HADD)</li> </ul>
<b>Inflammatory:</b> <ul style="list-style-type: none"> <li>• Seropositive                             <ul style="list-style-type: none"> <li>◦ Rheumatoid arthritis</li> </ul> </li> <li>• Seronegative                             <ul style="list-style-type: none"> <li>◦ Psoriatic arthritis</li> <li>◦ Ankylosing spondylitis</li> <li>◦ Enteropathic arthritis</li> <li>◦ Reactive arthritis</li> </ul> </li> <li>• Pediatric: Juvenile idiopathic arthritis</li> </ul>
<b>Infectious</b>
<b>Degenerative: Osteoarthritis</b>
<b>Connective tissue related and other miscellaneous arthropathies:</b> <ul style="list-style-type: none"> <li>• Systemic lupus erythematosus</li> <li>• Scleroderma</li> <li>• Adult-onset Still’s disease</li> <li>• Vasculitis</li> <li>• Sjögren’s syndrome</li> <li>• CNO; also known as SAPHO and CRMO</li> </ul>

Abbreviations: CNO, chronic nonbacterial osteomyelitis; CPPD, calcium pyrophosphate deposition disease; CRMO, chronic recurrent multifocal osteomyelitis; HADD, hydroxyapatite deposition disease; SAPHO, synovitis, acne, pustulosis, hyperostosis, osteitis.

This document was downloaded for personal use only. Unauthorized distribution is strictly prohibited.

Diagnosing gout hinges on identifying negatively birefringent MSU crystals in joint fluid or tophi through polarized microscopy.<sup>13,26</sup> However, this method is infrequently used in clinical practice due to its invasiveness and other limitations.<sup>13</sup> Imaging modalities that can facilitate the diagnosis of gout and are included in the American College of Rheumatology/European League Against Rheumatism (ACR/EULAR) criteria: plain radiography (presence of typical bone erosions), US (presence of a “double-contour” sign), and DECT (color-coded MSU crystals)<sup>27</sup> (► Fig. 6).

Characteristic radiographic findings are present only in the chronic stage, and therefore US is a common modality used to assess gout. Features of early and chronic gout on US are well described in the literature.<sup>26</sup> In early gout, joint effusions with or without hyperechoic MSU crystal foci may be seen that measure < 1 mm (“starry sky” sign). Larger MSU aggregates, referred to as micro-tophi, may result in a “snowstorm” appearance. The presence of MSU crystals embedded in hypertrophied synovium may increase the specificity.<sup>26</sup>

The double-contour sign results from deposition of gout crystals on the surface of the articular cartilage and results in a continuous hyperechoic line. It needs careful distinction from the “cartilage interface” sign that is a hyperechoic reflection at the cartilage border that appears only at a 180-degree angle. In chronic gout, the tophi appear as well

circumscribed, hyperechoic, or hypoechoic nodules that initially are uniform.<sup>26,28</sup> With chronicity, they become nonhomogeneous (“wet clumps of sugar” sign), with characteristic tiny internal hyperechoic echoes or aggregates. Juxta-articular erosions may also be seen.

The clinical use of DECT for the diagnosis of gout diagnosis has dramatically increased over the past decade, and its validity as a tool for the diagnosis has been established.<sup>13</sup> Based on reliable published data and its diagnostic accuracy,<sup>13</sup> DECT was incorporated into the 2015 ACR/EULAR gout classification criteria.

Sotniczuk et al assessed the diagnostic value of DECT in patients with a clinical suspicion of gout and compared the ACR/EULAR criteria with and without DECT diagnosis.<sup>27</sup> Considering artifacts, the combination of DECT and clinical findings resulted in the best diagnostic accuracy. Gamala et al conducted a meta-analysis of 10 studies on the diagnostic accuracy of DECT and revealed that the pooled sensitivity and specificity of DECT are 81% and 91%, respectively, whereas the pooled sensitivity was 55% in patients with recent-onset disease ( $\leq 6$  weeks).<sup>29</sup>

Other studies report sensitivities between 12% and 90%.<sup>13</sup> A systematic review in 2022 showed that DECT images are reliably interpreted with intra-rater intraclass correlation coefficients ranging from 0.86 to 1.00.<sup>30</sup> DECT overall had very good sensitivity and specificity in established gout

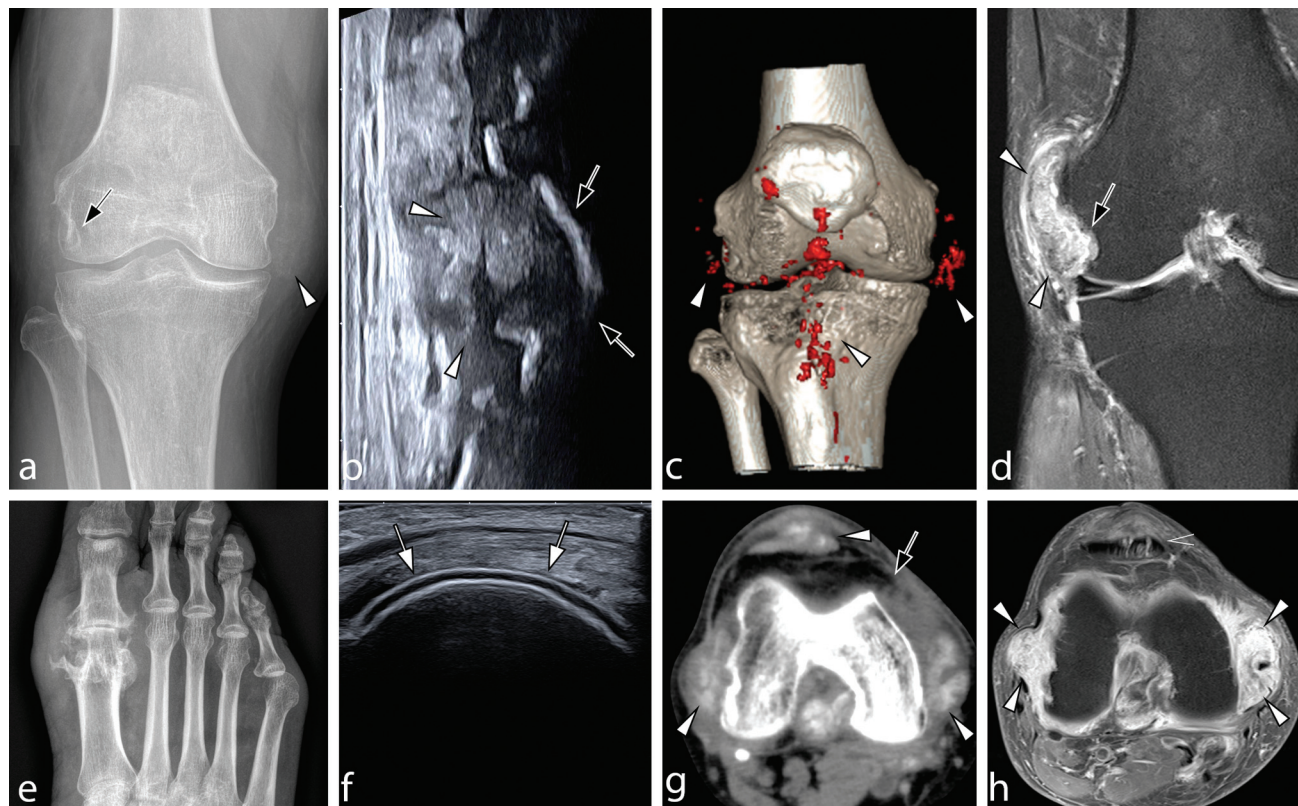


**Fig. 6** Patient evaluation for total knee arthroplasty. Erosion (black arrows) and tophus (white arrowheads) is better seen on ultrasonography (US) (b), computed tomography (CT) (g), and magnetic resonance imaging (MRI) proton-density fat-suppressed (FS) sequence (d) compared with radiography (a). Tophus is highlighted in dual-energy computed tomography (DECT) (c) and shows massive vascularization in contrast-enhanced T1 FS MRI (h). Sagittal US of the trochlea shows a typical double-contour sign (white arrowheads) (f). Note that small tophi in the patellar tendon are very well visualized by DECT and CT but not with MRI (open arrow). (e) Radiography of the forefoot shows typical gout lesions at the first metatarsophalangeal joint, illustrating the strength of radiography to image multiple joints with minimal effort.



when compared with joint aspiration, with ranges from 0.78 to 0.89 and 0.84 to 1.00, respectively. DECT also performed very well against clinical criteria, with a pooled sensitivity and specificity of 0.81 (95% confidence interval [CI], 0.77–0.86) and 0.91 (95% CI, 0.85–0.95).<sup>30</sup>

A study comparing the diagnostic accuracies of dual-source DECT and US in patients with different gouty disease durations reported that the sensitivities of DECT for gout within 1 year, 1 to 3 years, and > 3 years are 26.6%, 66.6%, and 90%, respectively.<sup>31</sup> They also revealed that the sensitivity of US is remarkably higher than that of dual-source DECT in early gout and suggested US as the first choice to diagnose early-stage gout.<sup>13</sup> Another research group reported a higher sensitivity of 80% using dual-source DECT in 20 gout patients with symptom duration < 6 weeks.<sup>13</sup> The outcomes demonstrated that disease duration strongly affects the diagnostic accuracy of single-source DECT, and DECT has limited diagnostic value in early-stage gout.

These results are attributable to the limitations of DECT in spatial (0.5–2 mm) and contrast resolution. Studies reported a concentration threshold of detectable MSU crystals between 20% and 35%.<sup>13,26,32</sup> In clinical practice, the concentration and detectability of MSU tophi is influenced by disease duration because it influences crystal volume and the active chemotaxis and phagocytosis of leukocytes.<sup>13</sup> Also, postcontrast intrinsic vascularization of tophi can increase its density, thus helping make low-concentration tophi visible.<sup>33</sup>

DECT may be used to stage patients with gout, especially in established disease, because 50% of patients have abnormal DECT scans with normal serum urate levels and no clinical tophi.<sup>30</sup>

Other applications of DECT include prediction of disease flares at 6 months and 2 years and excess cardiovascular and all-cause mortality.<sup>30</sup>

### Rheumatoid Arthritis

RA is a systemic autoimmune disease that predominantly affects the MSK system; the knee is one of the most commonly involved joints. It induces polyarthritis and inflammation in tendon sheaths and bursae. Chronic synovitis and osteitis contribute to the progressive destruction of hyaline cartilage, bone, and soft tissue.<sup>34,35</sup>

Early inflammatory changes, such as synovitis, tenosynovitis, bursitis, and osteitis (BME), can be observed on US and MRI, along with periarticular demineralization potentially progressing to generalized bone loss that will be seen on radiographs. Although enthesitis is not typical for RA, secondary involvement of the patellar tendon enthesitis due to deep infrapatellar bursitis is common.

Late imaging changes, indicative of joint damage, include inflammatory cysts, joint erosions, uniform narrowing of the joint space following hyaline cartilage damage, knee deformities, and secondary OA (– Fig. 7). Bone damage (cysts, erosions, hyaline cartilage loss) is initiated by the synovitis or osteitis or both through the outside-in and inside-out mechanism.<sup>36</sup>

Kondo et al explored the significant association between knee joint US parameters and synovial inflammatory factors

in RA, involving 44 patients, both treated ( $n=25$ ) and untreated ( $n=19$ ).<sup>37</sup> US images were quantitatively analyzed using gray-scale assessment of synovial hypertrophy and echogenicity and power Doppler for vascularity. The study found significant correlations between US synovial hypertrophy, power Doppler vascularity, and synovial fluid inflammatory cytokine levels in untreated patients.

Meng et al conducted a prospective analysis of 26 knee joints from 22 patients undergoing total knee arthroplasty for RA treatment, revealing that characteristic MRI features of advanced knee joint RA are damage to cartilage and menisci, attributed to synovium infiltration allowing inflammatory cell infiltration.<sup>38</sup> The most severe pathologic changes in cartilage were fibrosis, thinning, and destruction; in the menisci, fibrosis and engulfing calcified debris were most prominent. Chaplin observed areas of completely destroyed cartilage, often filled with soft granulation tissue, and significantly reduced or vanished menisci in 50 patients undergoing synovectomy for RA.<sup>39</sup> Kimura and Vainio also noted that the knee menisci underwent a more rapid degeneration process than the cartilage in 47 patients undergoing synovectomy for RA treatment.<sup>40</sup>

Sarcopenia, a prevalent extra-articular manifestation in RA patients, is currently defined through developing diagnostic criteria, with imaging techniques central to measuring or estimating muscle mass quality.<sup>41</sup> According to the European Working Group on Sarcopenia in Older People 2 consensus, dual-energy X-ray absorptiometry is the gold standard for confirming sarcopenia diagnosis; US is recognized for its accessibility, low cost, and ease of use.<sup>41</sup> Despite potential variables affecting US imaging, parameters like cross-sectional area (CSA) and volume measured using panoramic images offer reliability comparable with MRI.<sup>41</sup> Salaffi et al found that MRI-CSA-25 can differentiate between sarcopenic and non-sarcopenic RA patients, serving as an imaging biomarker of this condition.<sup>41</sup>

### Juvenile Idiopathic Arthritis

The knee is the most commonly involved joint in JIA.<sup>22,42</sup> Contrary to adult arthropathies, joint damage in most children appears late; instead, developmental disorders may occur and are typical for JIA.

Previous studies showed that synovial inflammation and joint effusion in JIA are closely related to clinical arthritis activity.<sup>42</sup> The study on BME as an important manifestation of early bone involvement in JIA is presently lacking.<sup>42</sup> Yang et al found a positive correlation between BME and synovial hypertrophy.<sup>42</sup> Older children and children with long disease duration had a higher risk for BME, which was commonly a late presentation and more likely involved the weight-bearing surfaces of the joint.<sup>42</sup> BME was accompanied by synovitis in all joints. There was no BME finding without synovitis in this study, and there was a positive relationship between them.<sup>42</sup>

This finding is consistent with the traditional pathogenesis hypothesis for JIA that suggests inflammation from synovitis results in cartilage damage, bone erosion, and eventually BME. The median duration of disease in the BME group was 9 months, significantly longer than that in

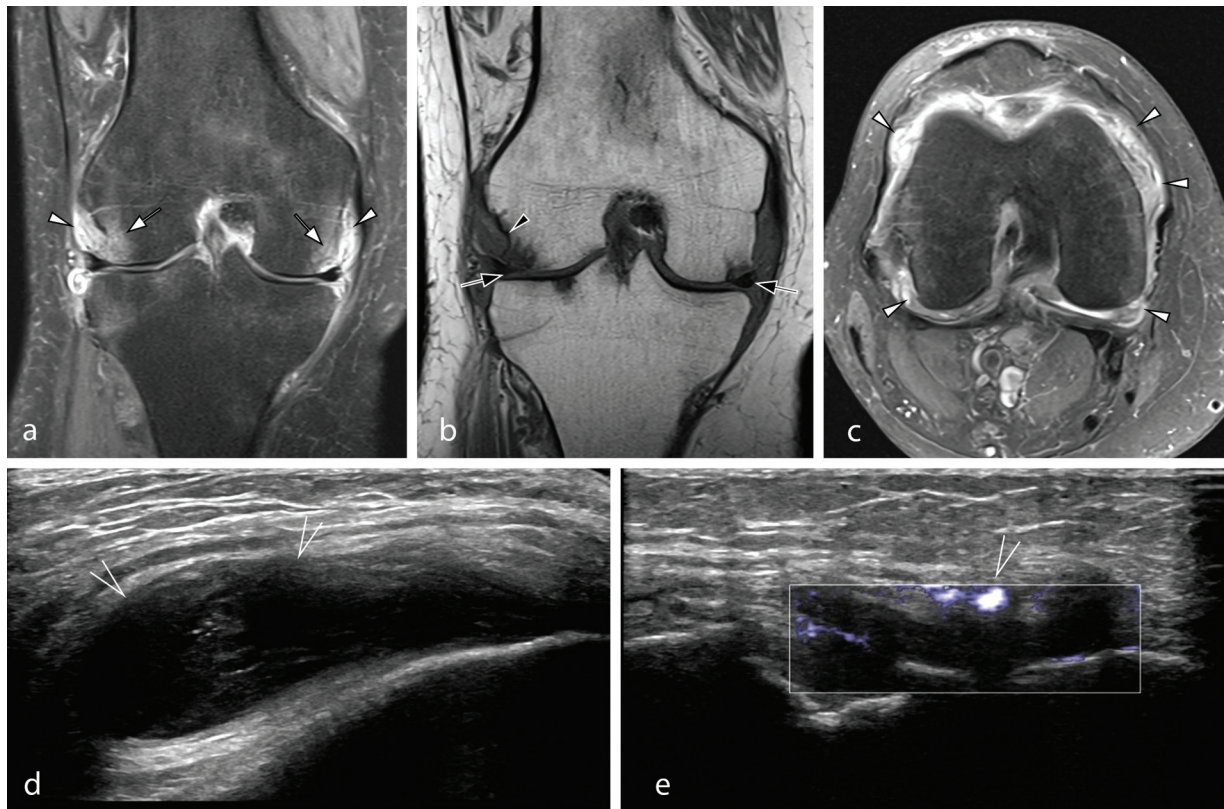


**Fig. 7** Knee magnetic resonance imaging (MRI) and ultrasonography (US) of a 47-year-old female patient with rheumatoid arthritis. MRI images: (a) coronal proton-density (PD) image with fat suppression (FS). (b) Coronal T1. (c) Axial proton-density FS. (e, f) Knee US. On MRI images, synovitis (white arrowheads) and bone marrow edema (white arrows), erosions (black arrowhead), and deep cartilage loss (black arrows) are seen. On US, effusion with (d) synovial thickening in the suprapatellar recess with vascularization is seen in (e), the medial compartment (open white arrows).

the non-BME group (4 months), suggesting that BME may not happen during the early JIA development but rather occurs gradually with the progression of JIA. This differs from adult RA where BME was reported more frequently in early disease development<sup>42</sup> (→ Fig. 8).

### Axial Spondyloarthritis

The most common form of axial SpA is ankylosis spondylitis (AS). In 10 to 20% of cases, the disease begins with asymmetric involvement of peripheral joints, predominantly affecting the knee and hip. Unlike RA, erosions are atypical and seldom



**Fig. 8** Knee magnetic resonance imaging of a 17-year-old girl with juvenile idiopathic arthritis (JIA). Proton-density with fat suppression images in (a) sagittal and (b) coronal planes, (c) T1 in coronal, and (d) T2 in sagittal planes. Effusion and synovitis (white arrows), subchondral bone marrow edema of the lateral femoral loaded part of the articular surface (white arrowheads), marginal erosions laterally (black arrow), grade 3 chondromalacia (open white arrow), menisci degeneration, with protrusion, lateral meniscus with a bucket-handle tear (b, c), dysmorphism of the joint secondary to JIA with hypoplasia of the femoral and tibial condyles and articular surfaces (b, c) and ankylosis in the tibiofibular joint (open black arrow).



**Fig. 9** A 35-year-old female patient with axial spondyloarthritis and knee pain. (a, b) Radiography shows mild effusion (white arrowheads). (c) Proton-density fat-suppressed magnetic resonance imaging (MRI) shows mild and diffuse bone marrow edema (white arrowheads). (d) After contrast administration, T1 fat-suppressed sagittal MRI depicts synovitis (black arrowheads). MRI of the sacroiliac joints with (e) T1 and (f) T2 fat-suppressed sequences shows active sacroiliitis (black arrows).

observed in most cases. Instead, periarticular soft tissue thickening, bone loss, uniform joint space narrowing, osteophytes, and isolated cysts, with enthesopathy a hallmark feature, are found. Other characteristic imaging findings for axial SpA include tenosynovitis, bursitis, and BME<sup>43–45</sup> (► Fig. 9).

In psoriatic arthritis, enthesopathy and periostitis may be seen in the knee. BME in the peripheral joints may be more diffuse than in other forms of SpA,<sup>46</sup> but this finding has not been assessed in the knee (► Fig. 10).

The knee and ankle joints are commonly involved in reactive and inflammatory bowel diseases associated with

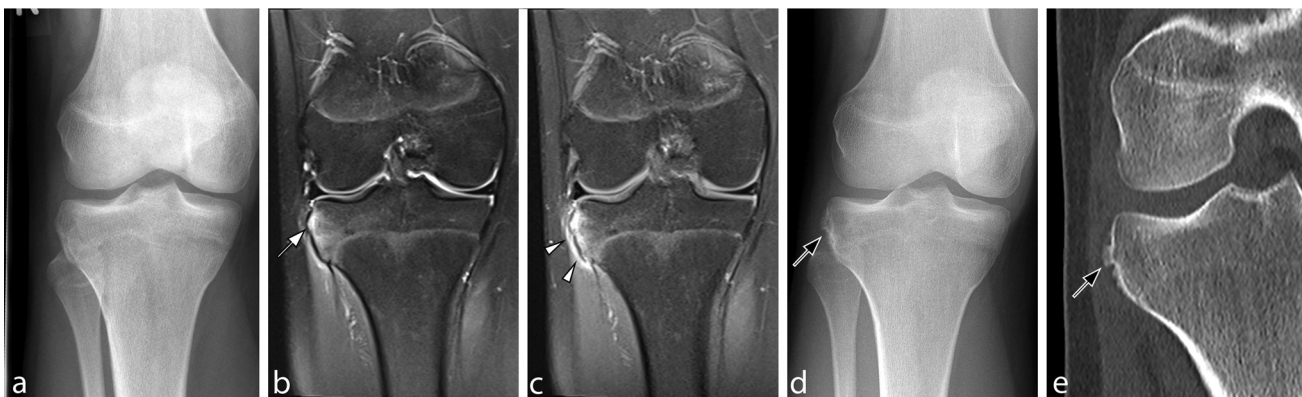


**Fig. 10** A 17-year-old female patient with psoriatic arthritis. (a) Initial radiography is unremarkable. However, (b) proton-density fat-suppressed magnetic resonance imaging shows bone marrow edema (white arrow). (c) It was also visualized after contrast enhancement in addition to pronounced soft tissue inflammation (white arrowheads). Follow-up (d) radiography and (e) computed tomography reveal new bone formation 1 year after symptom onset.

(enteropathic) arthritis.<sup>47</sup> The lesions include soft tissue thickening, periarticular bone loss, cysts, erosions, and periostitis/new bone formation. In reactive SpA, enthesopathic lesions are common, whereas in enteropathic SpA, imaging findings are similar to AS, described earlier.

### Scleroderma, Dermatomyositis, and Polymyositis

The diagnosis of inflammatory lesions in scleroderma in the skin, subcutaneous tissues, as well as in fascia and muscles (in deep scleroderma), is often performed by US. The last few years have seen a spectacular development in US, with the introduction of high-frequency probes, options for assessing microvascularity, and the use of SWE (►Fig. 2). These techniques enable early diagnosis, characterization, and quantification of disease activity and treatment monitoring<sup>48–51</sup> (►Fig. 2).

In the limited form as CREST syndrome (calcinosis, Raynaud's phenomenon, esophageal dysmotility, sclerodactyly, and telangiectasias) and in other forms like calcinosis universalis, calcifications of the subcutaneous tissue at certain points of mechanical stress may be best evaluated with radiography or CT.<sup>52–54</sup> MRI is the method of choice for assessing inflammatory changes in muscle and fascia in the course of dermatomyositis and polymyositis in adults and juveniles, showing

“edema-like” signal intensity in affected muscle, fascia, and subcutaneous tissue that correlates with disease activity<sup>48,50</sup> (►Fig. 11). MRI can help determine the biopsy site. In chronic stages, fatty degeneration, muscle atrophy, and calcifications may be seen.

### Adult-onset Still's Disease

Adult-onset Still's disease (AOSD) is a rare systemic inflammatory disease of the connective tissue that usually affects the knee and wrist.<sup>43,48</sup> Its etiology is unknown. The imaging features in the knee may resemble RA and include periarticular soft tissue thickening, periarticular demineralization, erosions, joint space narrowing, and early formation of bony ankylosis seen on radiography, with joint effusion, synovitis, or tenosynovitis seen on US and on MRI. The characteristic findings of AOSD on PET/CT are increased 18F-FDG accumulation in the spleen, bone marrow, and lymph nodes.<sup>55</sup>

### Pediatric and Adult Chronic Nonbacterial Osteitis

A new and as yet unpublished consensus introduces “chronic nonbacterial osteitis” (CNO) as the preferred term for a syndrome previously known as synovitis, acne, pustulosis, hyperostosis, and osteitis (SAPHO), given that many patients do not exhibit all or even most of the eponymous symptoms. In

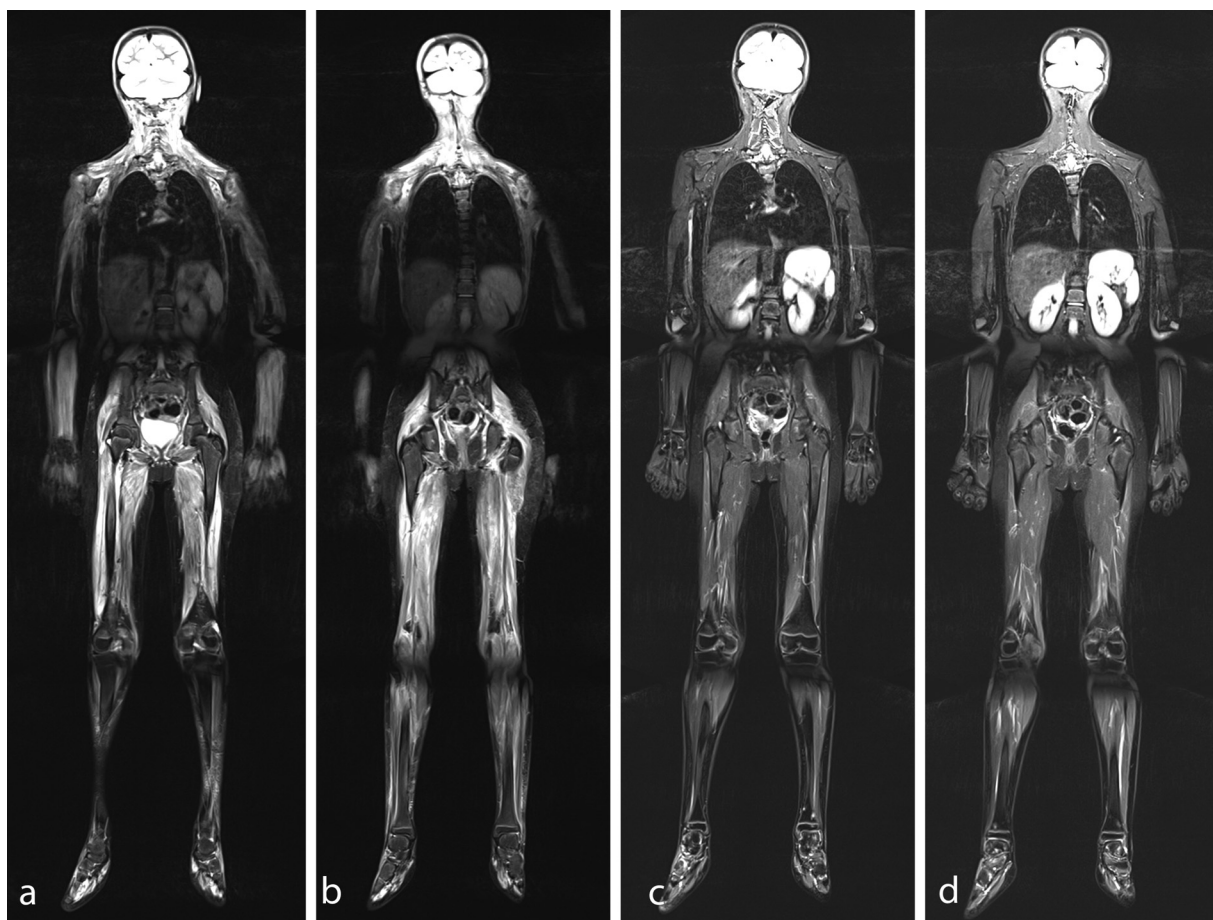


**Fig. 11** Whole-body magnetic resonance imaging in a 6-year-old girl with juvenile dermatomyositis, T2 turbo inversion recovery magnitude images in coronal planes. (a, b) Initial exam and (c, d) follow-up exam after 6 months of treatment. Initially seen high signal in numerous involved muscles of the neck, shoulder and pelvic girdles, and upper and lower limbs, including short muscles of the feet, undergo complete resolution after successful treatment.

children, the term CNO, or more specifically, chronic nonbacterial osteomyelitis, supersedes the former name CRMO (chronic recurrent multifocal osteomyelitis), acknowledging that not all patients meet the criteria for multifocality or recurrence. Although the etiology of CNO remains elusive, it is perceived as an autoinflammatory disease stemming from dysregulation of the innate immune system.<sup>56,57</sup>

Pediatric CNO, affecting children and adolescents, commonly affects the metaphyses of lower limb long bones (including those of the knee joint). In adults, where metaphyses are closed, the disease predominantly manifests in the anterior chest wall (specifically the sternoclavicular and sternomanubrial joints), the spine, and sacroiliac joints; peripheral joint involvement is rare.

Both pediatric and adult forms are characterized by excessive osteitis and periostitis, sometimes leading to peculiar new bone formation. Radiographs initially display bone lucency, progressing to sclerosis and new bone formation. Although MRI reveals active inflammation, it often fails to show periosteal new bone formation. Nevertheless, MRI, particularly WB-MRI, is the preferred method for early diagnosis in both children and adults (►Fig. 12).

In adult CNO, FDG-PET/CT has been used to evaluate sterile osteitis, and it can assist in evaluating treatment response by

identifying changes in FDG uptake and comparing SUVs. Although frequently recommended and occasionally indispensable, bone biopsy to rule out septic inflammation and abscesses is not always necessary.

## Conclusion

Over the past few decades, interest has been growing in novel imaging techniques for the assessment of inflammatory arthropathies.

In the context of suspected gouty arthritis, both US and DECT enable early diagnosis, each without proven superiority for initial assessment. Cost-effective US can reveal crystal depositions undetectable by DECT (e.g., the double-contour sign) and active inflammation manifested as synovitis with vascularization currently evaluated with even more sensitivity, thanks to microflow vascularity options. US also facilitates the planning or guidance of fluid aspiration or joint infiltration. Conversely, DECT offers standardized assessments suitable for follow-up, unveils tophi in areas inaccessible to US, and detects BME, potentially indicating active inflammation. DECT is also used for monitoring patients and evaluating treatment response. Both modalities are sensitive to bone erosion, a relatively late occurring but significant indicator of inflammatory arthritides.



**Fig. 12** A young boy with knee pain and chronic nonbacterial osteitis. (a, b) Radiography shows a lytic lesion associated with the epiphysis in the distal femur (white arrowheads) that is also visible in (c) magnetic resonance imaging (MRI) T1 and shows (d) surrounding bone marrow edema in the proton-density fat-suppressed sequence (open arrows). (e, f) Follow-up whole-body MRI reveals further lesions of the contralateral knee, the greater trochanter, and the acetabulum (black arrowheads) and another lesion of the thoracic spine with vertebral collapse (black arrow).

In patients with suspected RA of the knee, US and MRI offer a sensitive assessment of active and subclinical inflammation. MRI is easier to standardize and used increasingly in clinical trials, but more feasible US scores are in development to compensate this shortfall.<sup>58,59</sup>

For all autoimmune and/or autoinflammatory diseases, new imaging techniques are emerging, providing both qualitative and quantitative assessment of bone marrow, cartilage, tendons, and superficial tissues. As we have outlined in this review, many of these methods have been used successfully in the research setting. Others have already been incorporated in diagnostic algorithms, whereas incorporation of the remaining in clinical practice has been limited, and many challenges remain to be addressed.

#### Conflict of Interest

None declared.

#### References

- Sudoł-Szopińska I, Herregods N, Doria AS, et al. Advances in musculoskeletal imaging in juvenile idiopathic arthritis. *Biomedicine* 2022;10(10):2417
- Gitto S, Messina C, Vitale N, Albano D, Sconfienza LM. Quantitative musculoskeletal ultrasound. *Semin Musculoskelet Radiol* 2020;24(04):367–374
- Sudoł-Szopińska I, Jurik AG, Eshed I, et al. Recommendations of the ESSR Arthritis Subcommittee for the use of magnetic resonance imaging in musculoskeletal rheumatic diseases. *Semin Musculoskelet Radiol* 2015;19(04):396–411
- Mourad C, Cosentino A, Nicod Lalonde M, Omoumi P. Advances in bone marrow imaging: strengths and limitations from a clinical perspective. *Semin Musculoskelet Radiol* 2023;27(01):3–21
- Giraud C, Lecouvet FE, Cotten A, et al. Whole-body magnetic resonance imaging in inflammatory diseases: Where are we now? Results of an International Survey by the European Society of Musculoskeletal Radiology. *Eur J Radiol* 2021;136:109533
- Giraud C, Kainberger F, Boesen M, Trattnig S. Quantitative imaging in inflammatory arthritis: between tradition and innovation. *Semin Musculoskelet Radiol* 2020;24(04):337–354
- Vo Chieu VD, Vo Chieu V, Dressler F, et al. Juvenile idiopathic arthritis of the knee: is contrast needed to score disease activity when using an augmented MRI protocol comprising PD-weighted sequences? *Eur Radiol* 2023;33(05):3775–3784
- Barendregt AM, van Gulik EC, Groot PFC, et al. Prolonged time between intravenous contrast administration and image acquisition results in increased synovial thickness at magnetic resonance imaging in patients with juvenile idiopathic arthritis. *Pediatr Radiol* 2019;49(05):638–645
- Boesen M, Kubassova O, Sudoł-Szopińska I, et al. MR imaging of joint infection and inflammation with emphasis on dynamic contrast-enhanced MR imaging. *PET Clin* 2018;13(04):523–550
- Ezzati F, Chalian M, Pezeshk P. 3D MRI of the rheumatic diseases. *Semin Musculoskelet Radiol* 2021;25(03):425–432
- Altahawi F, Pierce J, Aslan M, Li X, Winalski CS, Subhas N. 3D MRI of the knee. *Semin Musculoskelet Radiol* 2021;25(03):455–467
- Sudoł-Szopińska I, Cotten A, Teh J. Foot and ankle inflammatory arthritis. In: Davies M, James S, Botchu R, eds. *Medical Radiology. Diagnostic Imaging. Imaging of the Foot & Ankle: Techniques and Applications*. 2nd ed. Cham, Switzerland: Springer; 2023: 355–390
- Shang J, Li XH, Lu SQ, Shang Y, Li LL, Liu B. Gout of feet and ankles in different disease durations: diagnostic value of single-source DECT and evaluation of urate deposition with a novel semi-quantitative DECT scoring system. *Adv Rheumatol* 2021;61(01):36
- Diekhoff T, Kiefer T, Stroux A, et al. Detection and characterization of crystal suspensions using single-source dual-energy computed tomography: a phantom model of crystal arthropathies. *Invest Radiol* 2015;50(04):255–260
- Kotlyarov M, Hermann KGA, Mews J, Hamm B, Diekhoff T. Development and validation of a quantitative method for estimation of the urate burden in patients with gouty arthritis using dual-energy computed tomography. *Eur Radiol* 2020;30(01): 404–412
- Rajiah P, Sundaram M, Subhas N. Dual-energy CT in musculoskeletal imaging: what is the role beyond gout? *AJR Am J Roentgenol* 2019;213(03):493–505
- Ziegeler K, Hermann S, Hermann KGA, Hamm B, Diekhoff T. Dual-energy CT in the differentiation of crystal depositions of the wrist: does it have added value? *Skeletal Radiol* 2020;49(05):707–713
- Caballero Motta LR, Anzola Alfaro AM, Janta I, et al. Radiosynovectomy in routine care: an old tool with modern applications. *Ther Adv Musculoskelet Dis* 2021;13:X211055309
- Gholamrezanezhad A, Basques K, Batouli A, Matcuk G, Alavi A, Jadvar H. Clinical nononcologic applications of PET/CT and PET/MRI in musculoskeletal, orthopedic, and rheumatologic imaging. *AJR Am J Roentgenol* 2018;210(06):W245–W263
- Mallinson PI, Reagan AC, Coupal T, Munk PL, Ouellette H, Nicolaou S. The distribution of urate deposition within the extremities in gout: a review of 148 dual-energy CT cases. *Skeletal Radiol* 2014;43(03):277–281
- Benjamin M, McGonagle D. The enthesis organ concept and its relevance to the spondyloarthropathies. *Adv Exp Med Biol* 2009; 649:57–70
- Pracoń G, Aparisi Gómez MP, Simoni P, Gietka P, Sudoł-Szopińska I. Conventional radiography and ultrasound imaging of rheumatic diseases affecting the pediatric population. *Semin Musculoskelet Radiol* 2021;25(01):68–81
- Dubash SR, De Marco G, Wakefield RJ, Tan AL, McGonagle D, Marzo-Ortega H. Ultrasound imaging in psoriatic arthritis: what have we learnt in the last five years? *Front Med (Lausanne)* 2020; 7:487
- Sudoł-Szopińska I, Kontny E, Zaniewicz-Kaniewska K, Prohorec-Sobieszek M, Saied F, Maśliński W. Role of inflammatory factors and adipose tissue in pathogenesis of rheumatoid arthritis and osteoarthritis. Part I: Rheumatoid adipose tissue. *J Ultrason* 2013; 13(53):192–201
- Michalski E, Ostrowska M, Gietka P, Sudoł-Szopińska I. Magnetic resonance imaging of the knee joint in juvenile idiopathic arthritis. *Reumatologia* 2020;58(06):416–423
- Sudoł-Szopińska I, Alfonso PD, Jacobson JA, Teh J. Imaging of gout: findings and pitfalls. A pictorial review. *Acta Reumatol Port* 2020; 45(01):20–25
- Sotniczuk M, Nowakowska-Płaza A, Wroński J, Wisłowska M, Sudoł-Szopińska I. The clinical utility of dual-energy computed tomography in the diagnosis of gout—a cross-sectional study. *J Clin Med* 2022;11(17):5249
- Lee YHGG, Song GG. Diagnostic accuracy of ultrasound in patients with gout: a meta-analysis. *Semin Arthritis Rheum* 2018;47(05): 703–709
- Gamala M, Jacobs JWG, van Laar JM. The diagnostic performance of dual energy CT for diagnosing gout: a systematic literature review and meta-analysis. *Rheumatology (Oxford)* 2019;58(12): 2117–2121
- Stauder SK, Peloso PM. Dual-energy computed tomography has additional prognostic value over clinical measures in gout including tophi: a systematic literature review. *J Rheumatol* 2022;49 (11):1256–1268
- Zhang B, Yang M, Wang H. Diagnostic value of ultrasound versus dual-energy computed tomography in patients with different stages of acute gouty arthritis. *Clin Rheumatol* 2020;39(05):1649–1653
- Diekhoff T, Kotlyarov M, Mews J, Hamm B, Hermann KGA. Iterative reconstruction may improve diagnosis of gout: an ex vivo (bio)

- phantom dual-energy computed tomography study. *Invest Radiol* 2018;53(01):6–12
- 33 Kotlyarov M, Mews J, Ulas ST, Ziegeler K, Hamm B, Diekhoff T. Influence of contrast medium on tophus detection using dual-energy CT: phantom study and clinical illustration. *Eur Radiol Exp* 2023;7(01):43
  - 34 Colebatch AN, Edwards CJ, Østergaard M, et al. EULAR recommendations for the use of imaging of the joints in the clinical management of rheumatoid arthritis. *Ann Rheum Dis* 2013;72(06):804–814
  - 35 Karasick D. Imaging of rheumatoid arthritis. In: Weissman BN, ed. *Imaging of Arthritis and Metabolic Bone Disease*. Philadelphia, PA: Saunders Elsevier; 2009:340–364
  - 36 Ostrowska M, Maśliński W, Prochorec-Sobieszek M, Nieciecki M, Sudoł-Szopińska I. Cartilage and bone damage in rheumatoid arthritis. *Reumatologia* 2018;56(02):111–120
  - 37 Kondo Y, Suzuki K, Inoue Y, et al. Significant association between joint ultrasonographic parameters and synovial inflammatory factors in rheumatoid arthritis. *Arthritis Res Ther* 2019;21(01):14
  - 38 Meng XH, Wang Z, Zhang XN, Xu J, Hu YC. Rheumatoid arthritis of knee joints: MRI-pathological correlation. *Orthop Surg* 2018;10(03):247–254
  - 39 Chaplin DM. The pattern of bone and cartilage damage in the rheumatoid knee. *J Bone Joint Surg Br* 1971;53(04):711–717
  - 40 Kimura C, Vainio K. The pattern of meniscus damage in the rheumatoid arthritis. *Arch Orthop Unfallchir* 1975;83(02):145–151
  - 41 Salaffi F, Carotti M, Polisenio AC, et al. Quantification of sarcopenia in patients with rheumatoid arthritis by measuring the cross-sectional area of the thigh muscles with magnetic resonance imaging. *Radiol Med (Torino)* 2023;128(05):578–587
  - 42 Yang JH, Kwon HH, Lee JK, Bang SY, Lee HS. Successful arthroscopic treatment of refractory and complicated popliteal cyst associated with rheumatoid arthritis in combination with osteoarthritis: case series and literature review. *Rheumatol Int* 2019;39(12):2177–2183
  - 43 Resnick D, Kransdorf MJ. Rheumatoid arthritis and related diseases. In: Resnick D, Kransdorf MJ, eds. *Bone and Joint Imaging*. Philadelphia, PA: Saunders Elsevier; 2005:209–254
  - 44 Brown AK. How to interpret plain radiographs in clinical practice. *Best Pract Res Clin Rheumatol* 2013;27(02):249–269
  - 45 Sudoł-Szopińska I, Zaniewicz-Kaniewska K, Saied F, Kunisz W, Smorawińska P, Włodkowska-Korytkowska M. The role of ultrasonography in the diagnosis of rheumatoid arthritis and peripheral spondyloarthropathies. *Pol J Radiol* 2014;79:59–63
  - 46 Tom S, Zhong Y, Cook R, Aydin SZ, Kaeley G, Eder L. Development of a preliminary ultrasonographic enthesitis score in psoriatic arthritis—GRAPPA ultrasound working group. *J Rheumatol* 2019;46(04):384–390
  - 47 Sudoł-Szopińska I, Kwiatkowska B, Kołodziejczak M. Musculoskeletal extraintestinal manifestations during the course of non-specific bowel diseases. *Pol Przegl Chir* 2013;85(11):669–675
  - 48 Jacques T, Sudoł-Szopińska I, Larkman N, O'Connor P, Cotten A. Musculoskeletal manifestations of non-RA connective tissue diseases: scleroderma, systemic lupus erythematosus, Still's disease, dermatomyositis/polymyositis, Sjögren's syndrome, and mixed connective tissue disease. *Semin Musculoskelet Radiol* 2018;22(02):166–179
  - 49 Fodor D, Rodriguez-Garcia SC, Cantisani V, et al. The EFSUMB guidelines and recommendations for musculoskeletal ultrasound. Part I: Extra-articular pathologies. *Ultraschall Med* 2022;43(01):34–57
  - 50 Sudoł-Szopińska I, Jacques T, Gietka P, Cotten A. Imaging in dermatomyositis in adults and children. *J Ultrason* 2020;20(80):e36–e42
  - 51 Idzior M, Sotniczuk M, Michalski E, Gietka P, Sudoł-Szopińska I. Ultrasonography, MRI and classic radiography of skin and MSK involvement in juvenile scleroderma. *J Ultrason* 2021;20(83):e311–e317
  - 52 Krusche M, Schneider U, Diekhoff T. Calcinosis universalis in systemic sclerosis. *Dtsch Arztebl Int* 2021;118(07):115
  - 53 Freire V, Becce F, Feydy A, et al. MDCT imaging of calcinosis in systemic sclerosis. *Clin Radiol* 2013;68(03):302–309
  - 54 Elahmar H, Feldman BM, Johnson SR. Management of calcinosis cutis in rheumatic diseases. *J Rheumatol* 2022;49(09):980–989
  - 55 Shimizu H, Nishioka H. <sup>18</sup>F-FDG PET-CT in adult-onset Still's disease. *BMJ Case Rep* 2021;14(03):e242717
  - 56 Jurik AG, Klicman RF, Simoni P, Robinson P, Teh J. SAPHO and CRMO: the value of imaging. *Semin Musculoskelet Radiol* 2018;22(02):207–224
  - 57 Rubenstein J. Seronegative spondyloarthropathies and SAPHO syndrome. In: Weissman BN, ed. *Imaging of Arthritis and Metabolic Bone Disease*. Philadelphia, PA: Saunders Elsevier; 2009:410–427
  - 58 Rakieh C, Nam JL, Hunt L, et al. Predicting the development of clinical arthritis in anti-CCP positive individuals with non-specific musculoskeletal symptoms: a prospective observational cohort study. *Ann Rheum Dis* 2015;74(09):1659–1666. Doi: 10.1136/annrheumdis-2014-205227
  - 59 Jaremko JL, Jeffery D, Buller M, et al. Preliminary validation of the Knee Inflammation MRI Scoring System (KIMRISS) for grading bone marrow lesions in osteoarthritis of the knee: data from the Osteoarthritis Initiative. *Ann Rheum Dis* 2015;74(06):1156–1163